CrossMark

Sulfate Resistance of Alkali Activated Pozzolans

Dali Bondar[1],*, C. J. Lynsdale[2], N. B. Milestone[3], and N. Hassani[4]

Abstract: The consequence of sulfate attack on geopolymer concrete, made from an alkali activated natural pozzolan (AANP) has been studied in this paper. Changes in the compressive strength, expansion and capillary water absorption of specimens have been investigated combined with phases determination by means of X-ray diffraction. At the end of present investigation which was to evaluate the performance of natural alumina silica based geopolymer concrete in sodium and magnesium sulfate solution, the loss of compressive strength and percentage of expansion of AANP concrete was recorded up to 19.4 % and 0.074, respectively.

Keywords: sulfate attack, geopolymer concrete, alkali activated natural pozzolan (AANP), X-ray diffraction, AANP concrete.

1. Introduction

When concrete is exposed in a solution containing a sufficiently high concentration of dissolved sulfates, the concrete deteriorates due to a series of chemical reactions. This is particularly prevalent in arid regions where naturally occurring sulfate minerals are present in water and ground water. Deterioration due to sulfate attack is generally attributed to reaction of hardened Portland cement hydration products with sulfate ions to form expansive reaction products after hardening, which produce internal stresses and a subsequent disruption of the concrete. It is generally accepted that sulfate ions attack the hydrated cement matrix by reaction of sulfate ions with the hydrated calcium aluminate phases along with $Ca(OH)_2$, forming ettringite and gypsum causing expansion of OPC concrete. Furthermore, with magnesium sulfate attack, brucite ($Mg(OH)_2$), which has low solubility, is produced and assumed to envelop the remainder of the cement gel and protect it against further deterioration. However, Turker reported that this process is only effective in the early stages of attack with deterioration due to brucite becoming dominant as the attack proceeds. Magnesium sulfate will also attack the C–S–H gel forming an M–S–H gel, which is non-cementitious and leads to softening of the cement matrix (Turker et al. 1997). In addition to chemical deterioration, salt crystallization, which usually involves repeated dissolution of the solid salt and re-crystallization, will occur in concrete pores and can be accompanied by large expansions and tension stresses far greater than the concrete bearing capacity (Ganjian and Pouya 2005). Concrete undergoing sulfate attack will suffer from swelling, spalling and cracking. The expansion leading to deterioration usually starts at edges and corners and is followed by progressive cracking with an irregular pattern. The lower the permeability of concrete is, the greater the resistance of concrete to sulfate attack. Thus, factors which reduce the permeability of concrete have a beneficial effect on reducing the vulnerability of concrete to sulfate attack.

Hakkinen evaluated the sulfate resistance of both alkali activated slag cement and Portland cement. The Portland cement samples were destroyed when exposed in 10 % Na_2SO_4 solution for 2 years or immersed in 10 % $MgSO_4$ solution for 1 year, while the alkali activated slag cement samples survived well (Hakkinen 1987, 1986).

Bakharev reported that concrete in which a geopolymer was the binder has a very different durability when exposed in sulfate solutions with the stability of the geopolymeric specimens tested depending on factors such as the type of activator used in specimen preparation, the concentration, and type of cation in the sulfate media. The results of the study are summarized in Table 1. The most significant deterioration reported was for exposure in a sodium sulfate solution where it appeared to be related to the migration of alkalies into solution. In a magnesium sulfate solution, migration of alkalies into the solution and magnesium and calcium diffusion to the subsurface areas was reported for a fly ash geopolymer

[1] Department of Civil, Architectural, and Building, Coventry University, Coventry CV1 5BF, UK.
*Corresponding Author; E-mail:
dlbondar@gmail.com;dali.bondar@coventry.ac.uk

[2] Department of Civil and Structural Engineering, University of Sheffield, Sheffield S1 3JD, UK.

[3] Milestone and Associates Ltd, Lower Hutt 5010, New Zealand.

[4] Research Centre of Natural Disasters in Industry, P.W.U.T., Tehran, Iran.

Table 1 Fluctuations of strength of fly ash based geopolymers in sodium and magnesium sulfate solutions, Bakharev (2005).

Immersed solutions	Activators	Fluctuations of strength
Sodium sulfate	Sodium hydroxide	4 % strength increase
	Sodium hydroxide and potassium hydroxide	65 % strength reduction
	Sodium silicate	18 % strength reduction
Magnesium sulfate	Sodium hydroxide	12 % strength increase
	Sodium hydroxide and potassium hydroxide	35 % strength increase
	Sodium silicate	24 % strength reduction

prepared using sodium silicate and a mixture of sodium and potassium hydroxides as activators (Bakharev 2005).

It was shown by Rangan (2008) that heat-cured, low calcium fly ash-based geopolymer concrete exhibited high resistance to sulfate immersion and attack. Specimens exposed in sodium sulfate for up to 1 year showed no visual signs of surface deterioration, cracking or spalling and compressive strength values remained equivalent to those obtained prior to immersion. Moreover, shrinkage was insignificant and was less than 0.015 % of the original dimensions (Rangan 2008).

Chotetanorm studied the resistance of high-calcium lignite bottom ash (BA) geopolymer mortars to sulfate attack. With median particle sizes of 16, 25, and 32 μm the BA was activated with NaOH or sodium silicate and temperature cured to prepare the geopolymer. Relatively high strengths of 40.0–54.5 MPa were obtained for the high-calcium BA geopolymer mortars with the use of fine BA improving the strength and resistance of mortars to sulfate attack. That superior performance was attributed to the high degree of reaction of fine BA giving rise to a low amount of large pores 0.05–100 μm compared with those of a coarse BA. The incorporation of additional water improved the workability of mixes, but the compressive strength, sorptivity, and resistance to sulfate attack decreased due to the increase in the numbers of large pores (Chotetanorm et al. 2013).

It seems that the use of the majority of pozzolans improves the sulfate resistance of mixes where geopolymer binders based on alkali activated natural pozzolans over that of ordinary Portland cement concrete. The simplest explanation for this is the lack of C_3A content, normally present if OPC was used (Bondar 2009). In geopolymer concrete the aluminates, that are prone to attack in OPC concrete along with monosulfate, are held in stable aluminosilicate hydrates which are more resistant to sulfate solutions. Secondly, in comparison with OPC, there is also much less calcium present in natural pozzolans to provide gypsum precipitation. In addition, the type of activator and the curing regime can affect the sulfate attack resistance of alkali activated pozzolan concrete mixture. The use of non-silicate alkaline activators increased the sulfate attack resistance of alkali-activated fly ash and slag cement in a $MgSO_4$ solution (Bakharev 2005; Shi et al. 2006) while steam curing of specimens made with water-glass with a modulus from 1 to 3 decreased the sulfate attack resistance compared to the specimens cured under normal conditions (Shi et al. 2006).

The objective of the present experimental program was to evaluate the performance of natural aluminosilicate based geopolymer concrete in sodium and magnesium sulfate solution. The focus of this paper is on sulfate resistance of alkali activated natural pozzolan concrete mixes and in this regard two types of pozzolanic materials (Taftan and Shahindej) were selected and the effect of two parameters including w/b ratio and different curing temperature and condition were just investigated for Taftan pozzolan. Shahindej pozzolan was studied as another type of natural pozzolan to show the effect of variety of material in raw and calcined form. The performance was assessed on the basis of compressive strengths, expansion and capillary water absorption of the specimens and combined with determination of phases formed discussed in this paper.

2. Experimental Work

2.1 Material and Mixing Procedure

Two natural pozzolans were used, Taftan andesite, the most reactive natural pozzolan in Iran, and Shahindej dacite, both of which are used to produce local Portland pozzolan cement. Optical microscopy showed that the Taftan pozzolan contained feldspar (sodic plagioclase, albite and hornblende), amphibole, quartz, and biotite, whereas Shahindej contained a sodium zeolite, clinoptilolite, albite, quartz and calcite (Ezatian 2002). By calcining Shahindej at 800 °C, the clinoptilolite was converted to opal which rapidly reacts with an alkaline solution (Bondar 2009). Calcination was not considered for Taftan pozzolan since it was applicable in ambient temperature in raw form but shahindej pozzolan needs calcinations to be applicable. Powder X-ray diffraction (XRD) was used to confirm the mineral compositions and the traces are presented in Fig. 1a–c. The chemical compositions were analysed using X-ray fluorescence (XRF) and are presented in Table 2 along with some physical properties.

Potassium hydroxide (KOH) pellets were dissolved in water to produce the alkaline solutions needed for geopolymer concrete production. Sodium silicate solution containing 8.5 % of sodium oxide (Na_2O), 26.5 % of silicon oxide (SiO_2) and 65 % of water; pH = 11.4 was used. The coarse aggregate used in this study was 14 mm and the fine sand 4.75 mm in size. The water absorption coefficient and

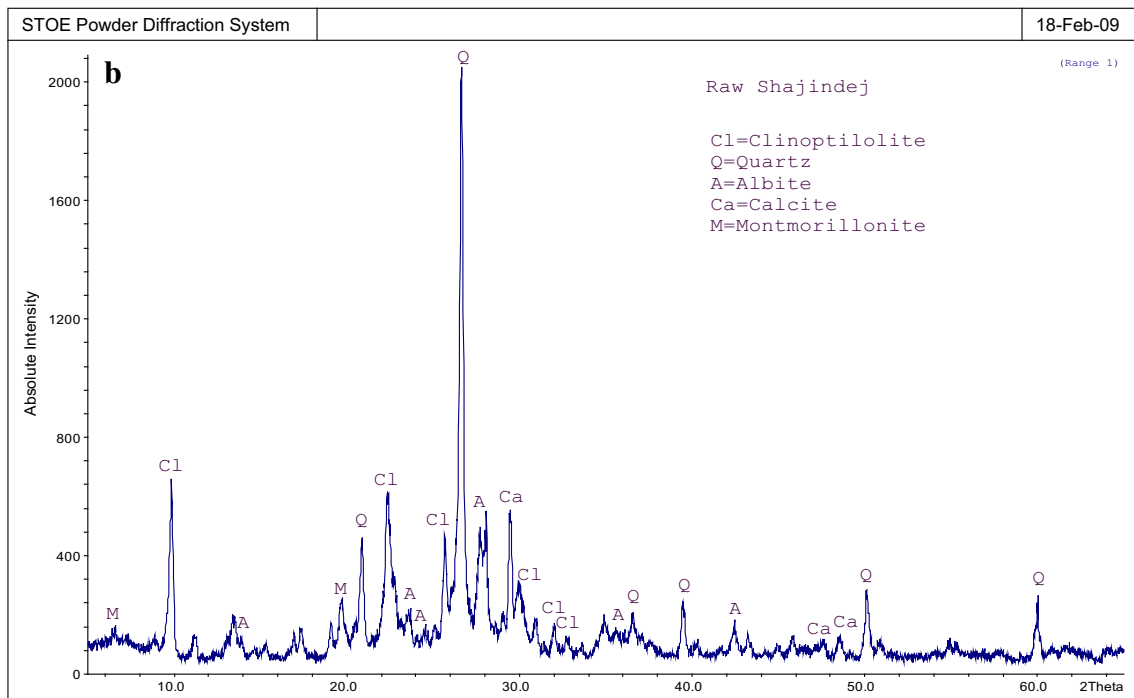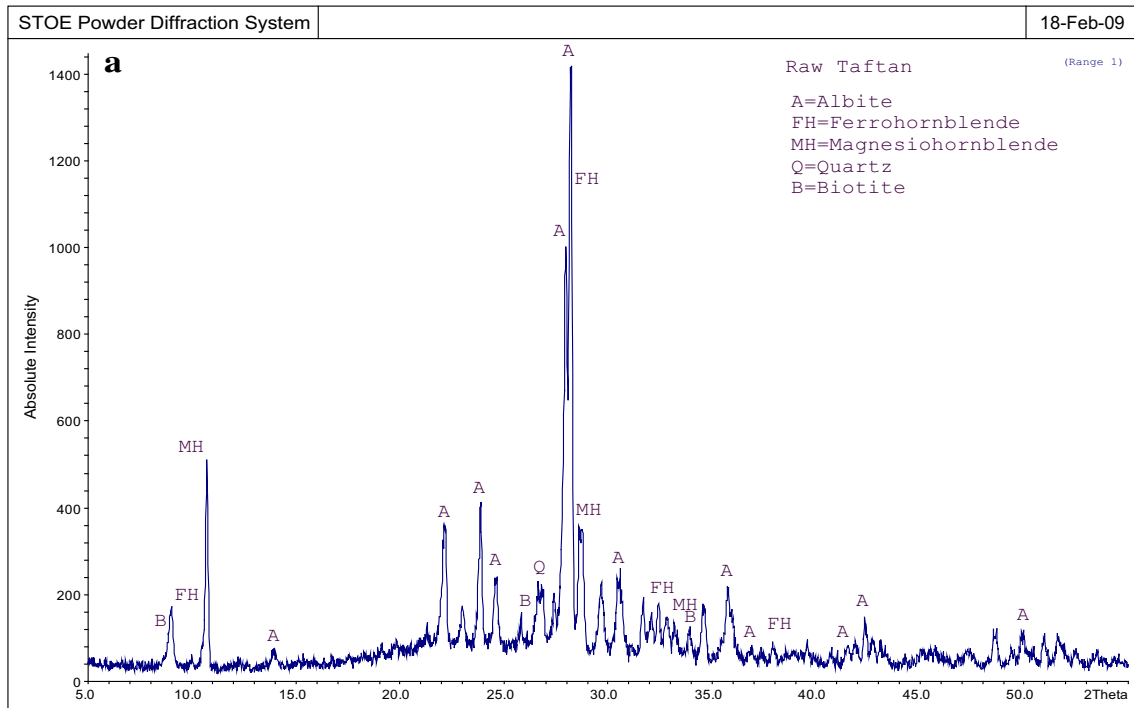**Fig. 1** **a** Mineralogical composition of Taftan andesite. **b** Mineralogical composition of Shahindej dacite. **c** Mineralogical composition of calcined Shahindej dacite.

bulk specific gravity of the saturated surface dry (SSD) aggregates were 0.6 % and 2.62 for the sand while for the gravel they were 0.9 % and 2.6. The fineness modulus of the combined aggregates used for making the concrete mixes was 2.8.

The proportions of the control concrete were based on the BRE (UK) method for design of normal concrete mixtures targeting a 40 MPa (28 days) compressive strength concrete with a slump of 60 mm (Neville 1995). The OPC binder was substituted with an equal quantity (by weight) of the natural pozzolan plus the solids in water

glass and the alkaline solution which was considered as the total binder to calculate the w/b. The mixture calculations including mix water, were made based on the optimum amount of activator needed to activate the pozzolan with no additional water added as the activators were already in solution (Bondar et al. 2011). The details of the different mixtures are presented in Table 3 and the notation for the mixtures is as follows:

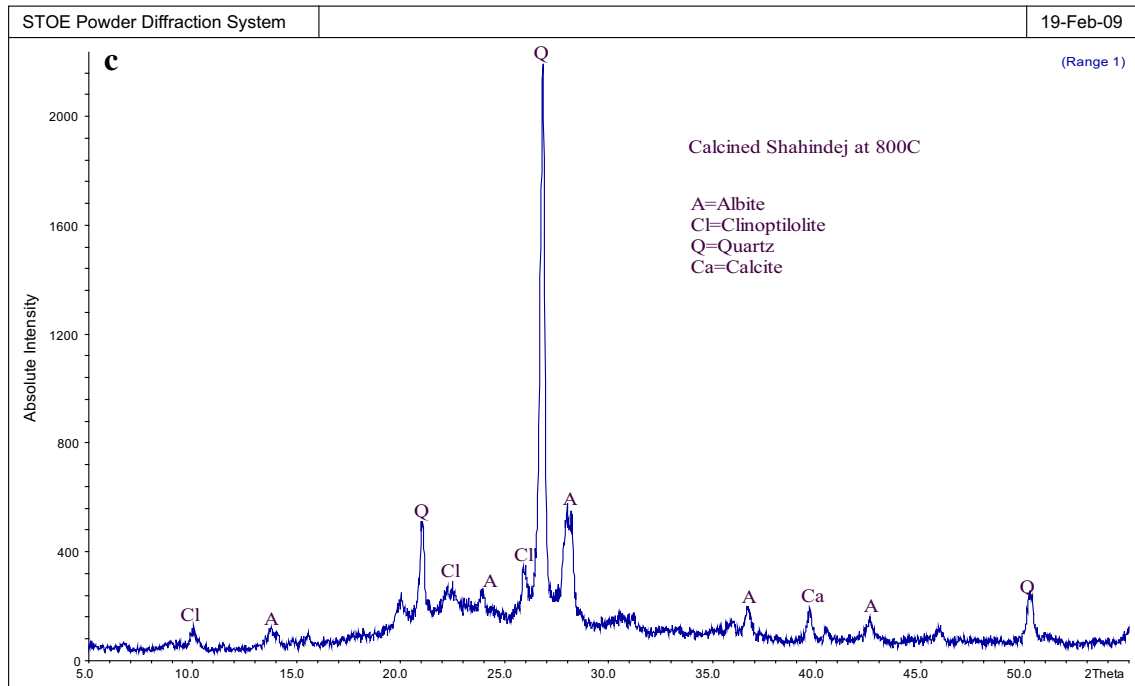ATAF1: Activated raw Taftan pozzolan mixture with w/b = 0.45.

c

(Range 1)

Calcined Shahindej at 800C

A=Albite
Cl=Clinoptilolite
Q=Quartz
Ca=Calcite

Fig. 1 continued

Table 2 Physical properties and chemical composition (oxide percent) of the materials used in this investigation.

Material	LOI (%)	SiO_2 (%)	Al_2O_3 (%)	Fe_2O_3 (%)	CaO (%)	MgO (%)	TiO_2 (%)	K_2O (%)	Na_2O (%)	Surface area (cm^2/g)	Specific gravity
Taftan andesite	1.85	61.67	15.90	4.32	7.99	2.04	0.44	2.12	3.21	3,836	2.22
Shahindej dacite	10.28	70.13	11.11	1.27	2.52	0.92	0.14	2.25	1.01	10,621	2.20
Shahindej dacite-800 °C	5.78	73.44	11.88	1.30	2.55	0.98	0.15	2.30	1.10	5,500	2.25

Table 3 Concrete mix proportion.

Mixture no.	Pozzolan (kg/m^3)	KOH (kg/m^3)	Na_2SiO_3 (cc/m^3)	Water (kg/m^3)	Total water (kg/m^3)	Total binder (kg/m^3)	Fine agg. (kg/m^3)	Coarse agg. (kg/m^3)	W/B %
ATAF1	325	66	34	158	180	403	578	1,229	0.45
ATAF2	272	72	37	171	195	357	702	1,121	0.55
ARSH	350	67	32	159	180	429	499	1,283	0.42
ACSH	350	67	32	159	180	429	499	1,283	0.42

ATAF2: Activated raw Taftan pozzolan mixture with w/b = 0.55.
ARSH: Activated raw Shahindej pozzolan mixture with w/b ratio = 0.42.
ACSH: Activated calcined Shahindej pozzolan mixture with w/b ratio = 0.42.

The concrete samples were cast in different sized moulds according to the tests described below. The mixtures were cast into pre-oiled moulds in three tamped layers and a vibrating table used to remove any entrapped air. It was observed that geopolymer concrete stuck to the mould and oiling of the moulds was very important to ensure release of the samples. Specimens were left at room temperature, covered by a plastic sheet and de-moulded after 24 h. Taftan specimens were exposed in two curing regimes and three different temperatures:

Table 4 Material type, curing regimes and exposure conditions for different mixes.

Mixture no.	Material type	Curing regime	Exposure conditions
ATAF1*	Raw Taftan	Sealed-20 °C	In a sulfate solution after 28 days curing (in)
			In curing regime till test date (out)
		Sealed-40 °C	In a sulfate solution after 28 days curing (in)
			In curing regime till test date (out)
		Fog-40 °C	In a sulfate solution after 28 days curing (in)
			In curing regime till test date (out)
		Sealed-60 °C	In a sulfate solution after 28 days curing (in)
			In curing regime till test date (out)
ATAF2	Raw Taftan	Sealed-20 °C	In a sulfate solution after 28 days curing (in)
			In curing regime till test date (out)
		Sealed-40 °C	In a sulfate solution after 28 days curing (in)
			In curing regime till test date (out)
		Fog-40 °C	In a sulfate solution after 28 days curing (in)
			In curing regime till test date (out)
		Sealed-60 °C	In a sulfate solution after 28 days curing (in)
			In curing regime till test date (out)
ARSH*	Raw Shahindej	Sealed-60 °C	In a sulfate solution after 28 days curing (in)
			In curing regime till test date (out)
ACSH*	Calcined Shahindej	Sealed-20 °C	In a sulfate solution after 28 days curing (in)
			In curing regime till test date (out)

* For expansion test one set of samples was put in pure water after 28 days curing in the related regime to compare the result with samples ponded in sulfate solution.

(1) *Sealed curing* Three series of specimens were closely wrapped in a special plastic covering shown to be impermeable to water and stored at controlled temperatures of 20 ± 2, 40 ± 2 and 60 ± 2 °C and less than 70 % RH.

(2) Fog curing at 40 ± 2 °C and 98 % RH was used for all of the measurements. To measure the changes of capillary water absorption of the specimens, fog curing at temperatures of 20 ± 2 and 60 ± 2 °C and 98 % RH was considered as well.

Raw and calcined Shahindej specimens both were all cured under sealed curing conditions. It was found that raw Shahindej pozzolan needed at least 60 °C curing to provide moderate to high strength at early stages while the optimum temperature for curing calcined Shahindej was found to be 20 °C. Therefore the ARSH concrete mixtures were cured at 60 °C and ACSH mixtures were cured at 20 °C and less than 70 % RH (Bondar 2009).

2.2 Sample Preparation and Test Method

Comparisons were made between specimens that had been immersed in a sulfate solution after 28 days curing and those that were cured as previously described in sealed or fog conditions till testing date. Material types, curing regimes and exposure conditions for different mixes were summarized in Table 4. Specimens were cast as 100 × 100 × 100 mm cubes (according to BS: 1881: part 116: 1983) for measuring the change of compressive strength and capillary water absorption and as 75 × 75 × 285 mm concrete prisms (according to ASTM C 490) in order to measure the

expansion. After de-moulding, the samples were cured as described above using the different curing conditions and temperatures for 28 days. The specimens were then immersed in a solution containing 2.5 % Na_2SO_4 and 2.5 % $MgSO_4$ by weight of water. The samples were placed in containers and left in a temperature controlled room at 20 °C for 6 months with some samples being retained for measuring changes of compressive strength over 2 years. The container solutions were replaced every 2 weeks for the first 3 months and then retained.

2.3 Test Procedure

The methods which test sulfate attack, are designed to assess four properties:

- changes in capillary water absorption (in accordance with the method specified by RILEM-CPC-11.2) (RILEM 1994) and
- compressive strengths of the specimens (according to BS: 1881: part 116: 1983),
- dimensional changes of the specimens which was measured according to ASTM C1012-95a (Astm and 1012–95a 1995), and
- the chemical phases using XRD.

2.4 Water Absorption and Compressive Strength

To assess the variations in capillary water absorption and compressive strength between specimens subjected to sulfate attack and those cured normally in sealed or fog conditions, 100 mm concrete cubes were cast and cured under the different curing conditions. Water absorption measurements were made at different ages up to 180 days for samples exposed in tap water (Na = 105, K = 30, Ca = 120, Mg = 50, Cl = 225, SO_4 = 85 ppm) and to the sulfate solution. In the test procedure specimens were dried to constant weight, the weight noted and the samples were then immersed in tap water or the sulfate solution. At specified times; samples were removed and weighed again. Absorption is expressed as the increase in weight as a percentage of the original weight.

The compressive strength of samples that had been exposed both in and out of the sulfate solution were measured periodically up to 2 years to examine the changes in the strength of cubes exposed in the sulfate solution and those left to cure normally in sealed or fog conditions. For any one mix and age, three cubes were tested.

2.5 Expansion Test

To measure rates of expansion, $75 \times 75 \times 285$ mm concrete prisms were prepared, exposed in sulfate solution and measured (One reference prism was exposed in pure water in order to compare the measurements). The amount of the expansion was calculated by measuring the specimens' length using the length comparator. For each mix three specimens were tested.

2.6 X-ray Diffraction Test

XRD was used to identify the crystalline products present in samples after they had been immersed in sulfate solution for up to 90 days. For analysis, a thin layer 0–5 mm in depth was carefully ground from the sample surface and examined by powder XRD. Its XRD trace was compared to that obtained for a powder prepared from a sample taken from the middle of the sample. This showed there was a difference in phases between the centre and edge of the sample after immersion in sulfate solution.

3. Results and Discussion

The percentage of water absorption for concrete specimens immersed in tap water and sulfate solutions for 180 days are presented in Fig. 2. All specimens recorded an increase in weight over the duration of exposure. The pattern of weight gain is similar in the two series of alkali activated Taftan pozzolan for the various curing regimes. The maximum increase in weight was observed for the ATAF1 specimen (w/b = 0.45) cured at 60 °C and the least gain in weight for the ATAF2 specimen (w/b = 0.55) cured at 20 °C under sealed conditions. The weight gain across all specimens was in the range of 5.1–7.0 %. The increase in weight of ATAF2
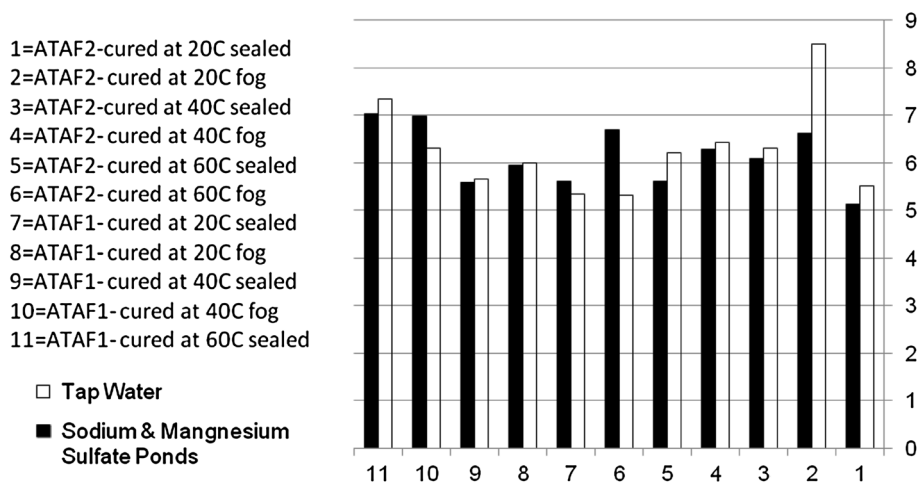

1=ATAF2-cured at 20C sealed
2=ATAF2-cured at 20C fog
3=ATAF2-cured at 40C sealed
4=ATAF2-cured at 40C fog
5=ATAF2-cured at 60C sealed
6=ATAF2-cured at 60C fog
7=ATAF1-cured at 20C sealed
8=ATAF1-cured at 20C fog
9=ATAF1-cured at 40C sealed
10=ATAF1-cured at 40C fog
11=ATAF1-cured at 60C sealed

□ Tap Water

■ Sodium & Mangnesium Sulfate Ponds

Fig. 2 Water absorption (in percent) in AANP concretes exposed in tap water and sodium & magnesium sulfate ponds.
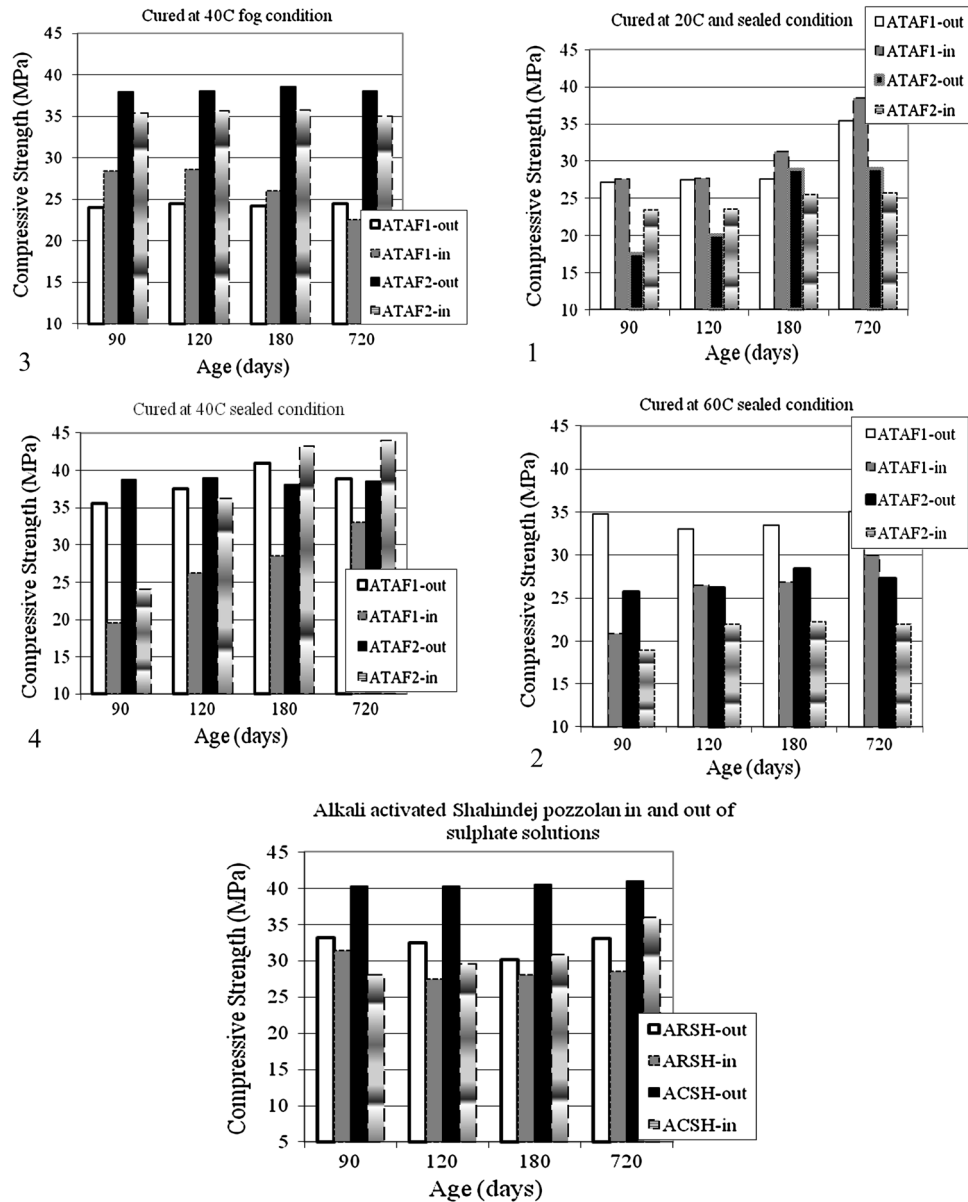
Fig. 3 Compressive strength for ATAF1 and ATAF2 mixes cured under different condition and temperatures, ARSH, and ACSH in and out of the sulfate solution.

specimens in sulfate solution for w/b = 0.55 cured at 60 °C in fog curing condition and ATAF1 specimen (w/b = 0.45) cured at 20 °C in sealed and at 40 °C in fog curing condition was more than the specimens immersed in tap water which might be due to white deposit within the surface pores. Higher amounts of absorption were recorded for all of the fog cured samples which may be due to a more open microstructure. For these samples permeability was higher than for comparable samples cured in a sealed condition (Bondar et al. 2012). Although the water in the geopolymer structure is just a medium that promotes the geopolymerization with further cross linking (Si–O–Al or Si–O–Si bonding) and poly condensation made, the phenomenon is related to more water being retained in the pores, resulting in a more porous microstructure giving rise to higher absorption and follows that found by Zuhua et al. (2009) for calcined kaolin-based geopolymer.

Figure 3 represents the evolution over time of compressive strengths for AANP concrete specimens that are exposed in the sulfate solutions after being cured for 28 days in a specific regime and specimens cured with same curing regime till testing date. The compressive strength results for each case were determined from average of three cubes. It seems there would be the movement of sulfate into the geopolymer. This is related to the absorption capacity of the geopolymer and thus the one absorbed more would have a large amount of sulfate in the matrix and hence affects the strength and the expansion. The strength of all sulfate cured concretes at 180 days was less than that for the samples cured outside of the solution initially, with the exception of the ATAF1 samples cured at 20 °C in sealed and 40 °C fog conditions and the ATAF2 samples cured at 40 °C in sealed conditions. The trend of compressive strength development is to increase, except for Taftan samples cured at 40 °C under fog
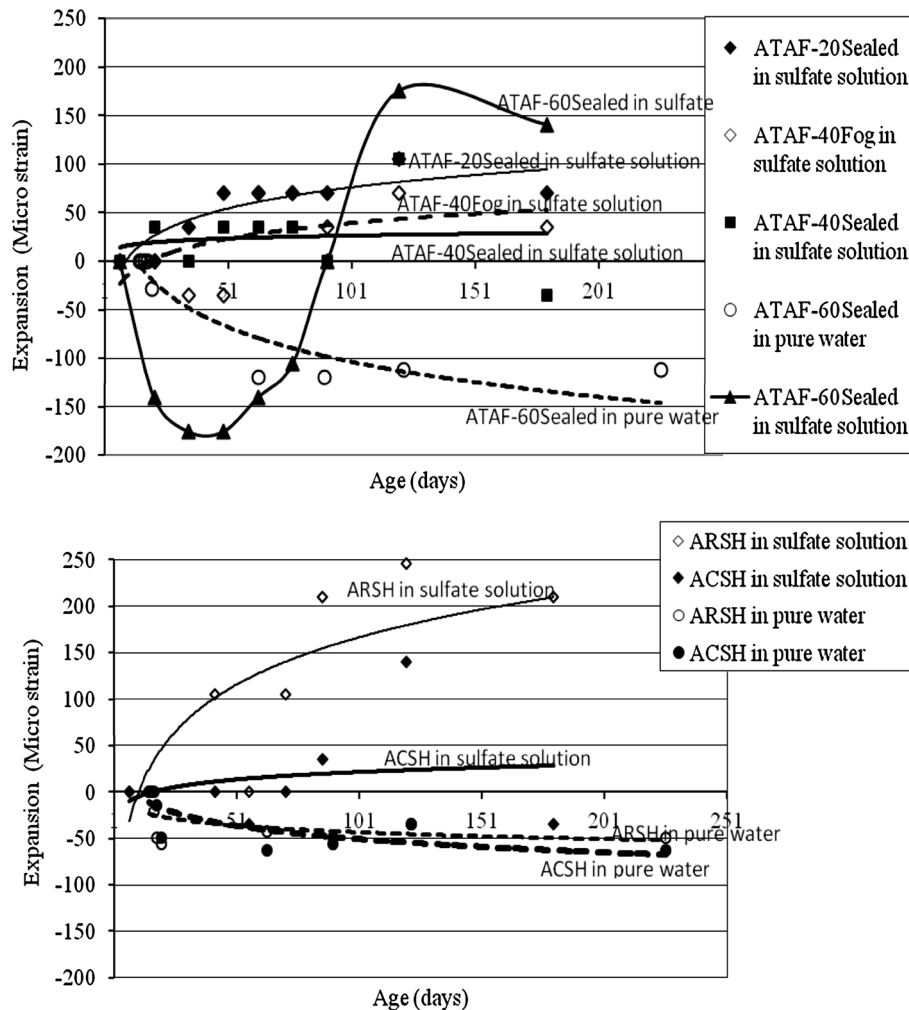
Fig. 4 Expansion at various ages for geopolymer mortar mixes based on alkali activated natural pozzolan in sulfate solution.

conditions and ARSH concrete mixes at this age. The results confirm previous investigations carried out on alkali activated cements (Bakharev 2005; Bakhareva et al. 2002). Lower w/b ratio resulted in higher strength for corresponding specimens that were exposed inside and outside of the sulfate solutions. However, a longer period of exposure to aggressive solutions was conducted to confirm the sulfate resistance of AANP concrete. The strength of all sulfate exposure AANP concrete samples was 8–19.5 % less than those cured outside of the solution by immersing samples for 2 years with the exception of Taftan samples with w/c = 0.45 cured at 20 °C under sealed conditions and Taftan samples with a w/c = 0.55 cure at 40 °C sealed conditions. For these samples, the strength of all sulfate cured concrete was 8.5 and 14 % more than the samples cured outside of the solution, respectively. For 5 months sulfate cured OPC concrete exposed to the same regime, the loss of strength was up to 38 % (Bakharev 2005).

The results of expansion tests against time are shown in Fig. 4. Alkali activated natural pozzolan which has the structure similar to zeolite, partly dehydrates, losing a part of its water molecules at ambient temperatures when the humidity drops below about 60 % and then rehydrates back

form when saturated with water. This reversible hydration associated with wetting and drying is accompanied by a volume change which is sufficient to cause expansion and shrinkage effects in structures which is obvious for Taftan samples cured at 60 °C under sealed conditions. The highest absolute expansion was recorded for the ARSH mortar prism which was most affected by sulfate solution and the lowest amount was recorded for ATAF cured at 40 °C and sealed condition after 6 months immersion. This follows the strength patterns reported previously (Bondar et al. 2011), and may be due to more geopolymer solids in the system causing lower permeability and a decrease of the penetration of sulfate ions so fewer expansive products are formed. The maximum expansion recorded for AANP concrete in this investigation was 0.074 % after 6 months immersion. Swamy reported that very poor durability was shown by OPC samples prepared at w/c = 0.45 and immersed in a sulfate solution. The highest expansion was recorded as 0.25 and 0.35 % for OPC samples immersed in Na and Mg sulfate solutions for 42 days, respectively (Swamy 1998). The maximum percentage of expansion recorded for ARSH mixes was 0.086 % at 6 months and the trend is for this to decrease after this time. Therefore the maximum percentage

expansion measured for AANP concrete in this study is less than the 0.1 % which ASTM C1012 Standard (Astm and 1012–95a 1995) suggests as acceptable for OPC concretes in moderate sulfate exposure conditions at 6 months and later.

The crystalline reaction compounds taken from surfaces and middles of cubes were analysed by XRD and the phases present are shown in Fig. 5a–c and summarized in Table 5. It can be seen that the peaks for the reaction products taken from the surface of alkali activated natural pozzolan mortar specimens, are higher than for the same compounds taken from the middle of cubes, after 3 month exposure in the sulfate solutions. For the activated Taftan samples the main crystalline compounds present in both the surface and middle part of specimens were albite (Na-AlSi$_3$O$_8$) and quartz (SiO$_2$) with hornblende and clinoptilolite present for the activated Shahindej samples. The
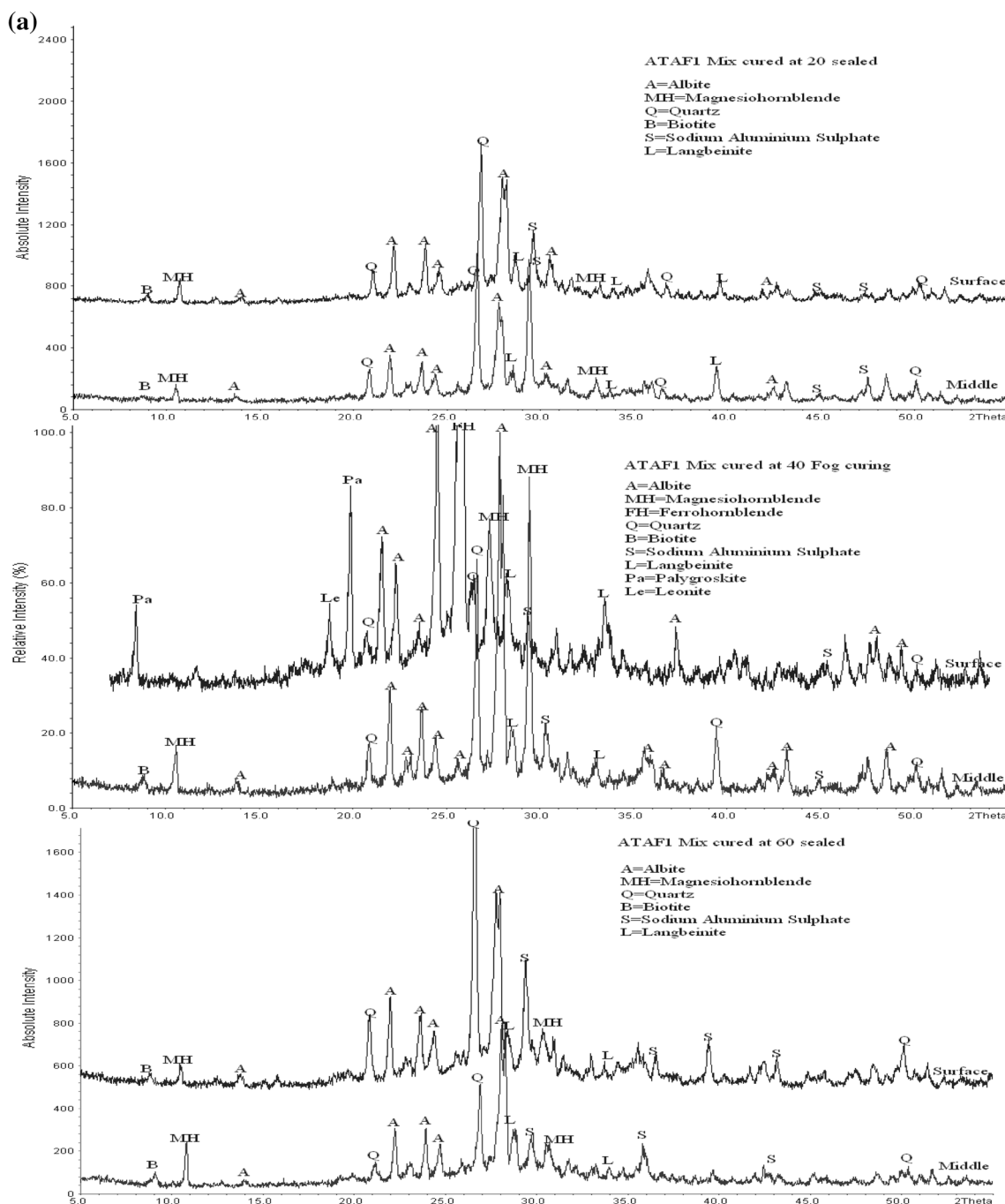
Fig. 5 **a** X-ray diffraction results show the existence of sulfate phases achieved from the powder prepared from the surface and the middle of the samples of ATAF1 mixtures cured at 20 ± 2, 40 ± 2 and 60 ± 2 °C and immersed in sulfate solution. **b** X-ray diffraction results show the existence of sulfate phases and achieved from the powder prepared from the surface and the middle of the samples of ATAF2 mixtures cured at 40 ± 2 and 60 ± 2 °C immersed in sulfate solution. **c** X-ray diffraction results show the existence of sulfate phases and achieved from the powder prepared from the surface and the middle of the samples of ARSH mixtures cured at 60 ± 2 °C and ACSH mixtures cured at 20 ± 2 °C immersed in sulfate solution.
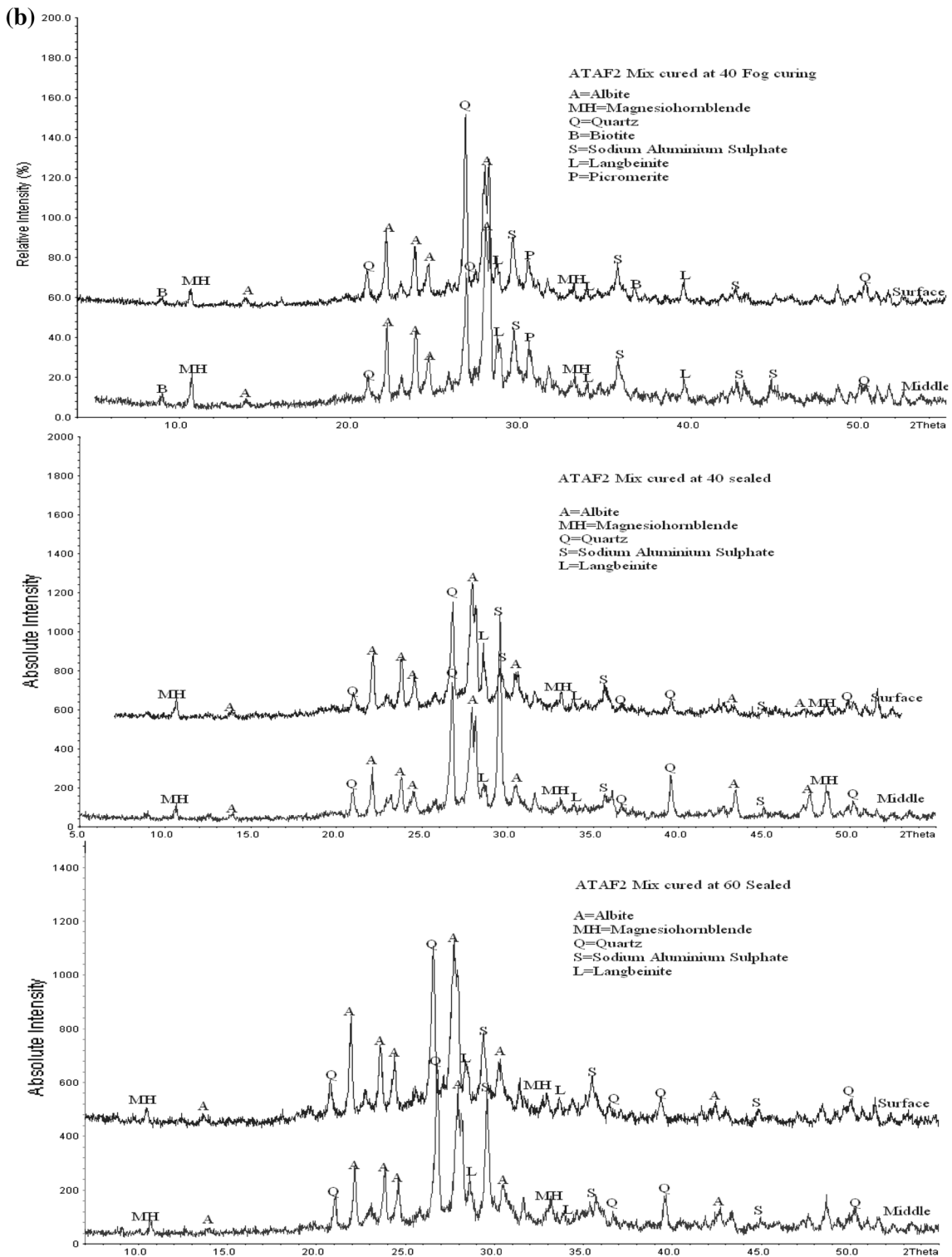
(b)

Fig. 5 continued

reaction products consisted mostly of sodium aluminium sulfate [$Na_3Al(SO_4)_3$] and/or langbeinite [$K_2Mg_2(SO_4)_3$] which may cause expansion in this type of concrete particularly at the edge of the samples. By comparing the X-ray traces of samples taken from the surface with those from the middle of the specimen shows that for activated, calcined Shahindej samples, the penetration of sulfate is very limited while for the activated, raw Shahindej, the peaks only relate to sodium aluminium sulfate. For the ATAF1 mix cured at 40 °C some hydrated sulfate salts such as leonite [$K_2Mg(SO_4)_2.4H_2O$] were detected on the surface of samples. Although the intensity of sulfate crystalline compound peaks in the middle of the specimens is lower than what was found for the surface of the specimens, the results show that in this type of concrete, sulfate could penetrate in the concrete. This can be confirmed
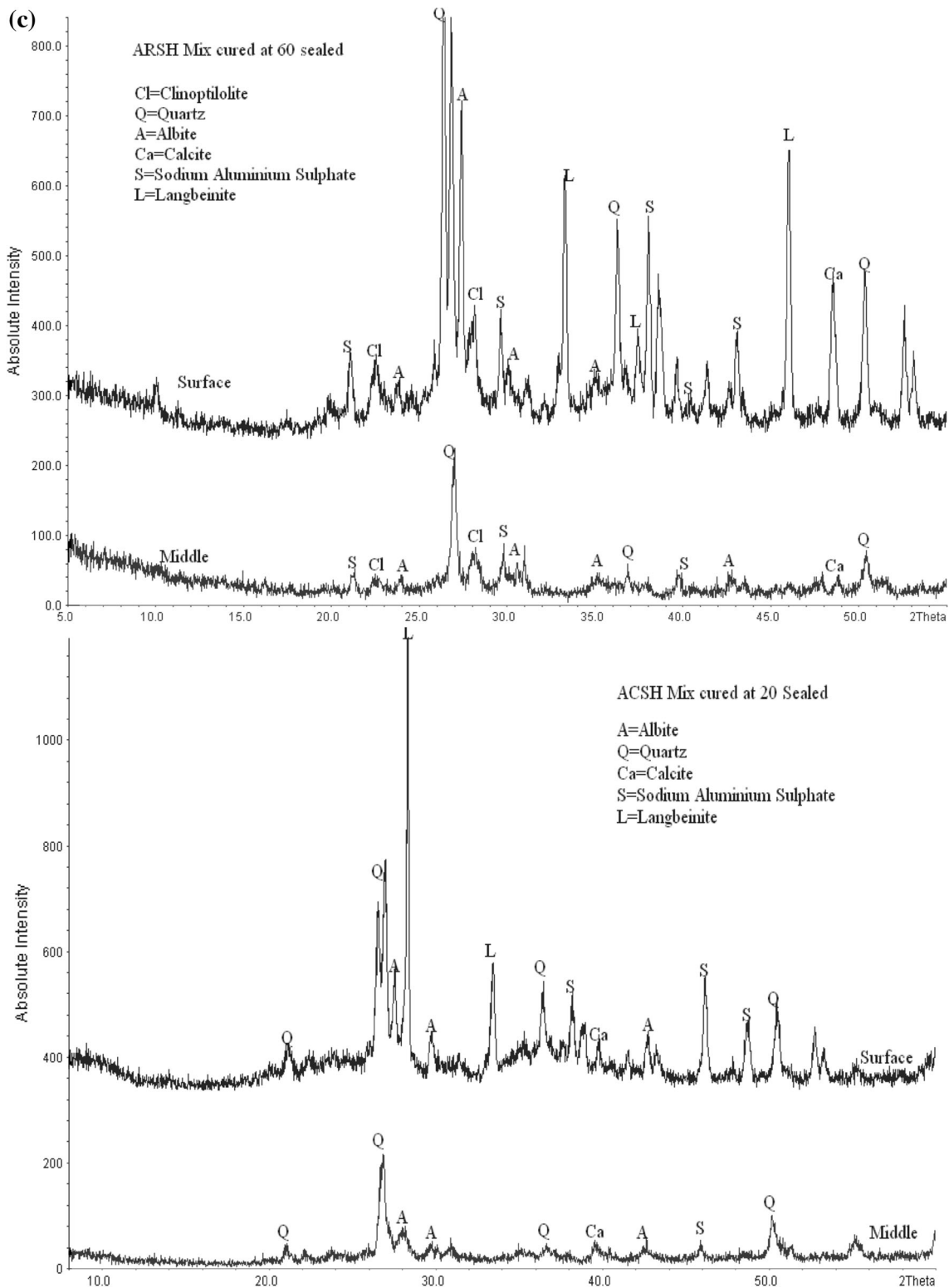
Fig. 5 continued

since the trace of sulfate combination was present in the core of all samples except ACSH. However, further studies exposing samples for 2 years in sulfate solution and strength measurement, has shown that the crystalline products formed in sulfate cured samples do not greatly reduce the resistance of AANP concrete.

Table 5 Summary of X-ray diffraction results show the existence of sulfate phases and achieved from the powder prepared from the surface and the middle of the samples immersed in sulfate solution.

Mix	Water to binder ratio (W/B)	Curing condition and temperature	Position of sampling	Sulfate phases	Mineral name of sulfate phases
ATAF1	0.45	Sealed curing at 20 °C	Surface	$Na_3Al(SO_4)_3$	Sodium aluminium sulfate
				$K_2Mg_2(SO_4)_3$	Langbeinite
ATAF1	0.45	Sealed curing at 20 °C	Middle	$Na_3Al(SO_4)_3$	Sodium aluminium sulfate
				$K_2Mg_2(SO_4)_3$	Langbeinite
ATAF1	0.45	Fog curing at 40 °C	Surface	$Na_3Al(SO_4)_3$	Sodium aluminium sulfate
				$K_2Mg_2(SO_4)_3$	Langbeinite
				$(MgAl)_5(SiAl)_8O_{20}(OH)_2 \cdot 8H_2O$	Palyigorskite
				$K_2Mg(SO_4)_2 \cdot 4H_2O$	Leonite
ATAF1	0.45	Fog curing at 40 °C	Middle	$Na_3Al(SO_4)_3$	Sodium aluminium sulfate
				$K_2Mg_2(SO_4)_3$	Langbeinite
ATAF1	0.45	Sealed curing at 40 °C	Surface	$Na_3Al(SO_4)_3$	Sodium aluminium sulfate
				$K_2Mg_2(SO_4)_3$	Langbeinite
				$(MgAl)_5(SiAl)_8O_{20}(OH)_2 \cdot 8H_2O$	Palyigorskite
				$K_2Mg(SO_4)_2 \cdot 4H_2O$	Leonite
ATAF1	0.45	Fog curing at 40 °C	Middle	$Na_3Al(SO_4)_3$	Sodium aluminium sulfate
				$K_2Mg_2(SO_4)_3$	Langbeinite
ATAF1	0.45	Sealed curing at 40 °C	Surface	$Na_3Al(SO_4)_3$	Sodium aluminium sulfate
				$K_2Mg_2(SO_4)_3$	Langbeinite
ATAF1	0.45	Sealed curing at 60 °C	Middle	$Na_3Al SO_4)_3$	Sodium aluminium sulfate
				$K_2Mg_2(SO_4)_3$	Langbeinite
ATAF2	0.55	Fog curing at 40 °C	Surface	$Na_3Al(SO_4)_3$	Sodium aluminium sulfate
				$K_2Mg_2(SO_4)_2 \cdot 6H_2O$	Picromerite
ATAF2	0.55	Fog curing at 40 °C	Middle	$Na_3Al(SO_4)$	Sodium
				$K_2Mg_2(SO_4)_3$	Langbeinite
				$K_2Mg(SO4)_2 \cdot 6H_2O$	Picromerite

Table 5 continued

Mix	Water to binder ratio (W/B)	Curing condition and temperature	Position of sampling	Sulfate phases	Mineral name of sulfate phases
ATAF2	0.55	Sealed curing at 40 °C	Surface	$Na_3Al(SO_4)_3$	Sodium aluminium sulfate
				$K_2Mg_2(SO_4)_3$	Langbeinite
ATAF2	0.55	Sealed curing at 40 °C	Middle	$Na_3Al(SO_4)_3$	Sodium aluminium sulfate
				$K_2Mg_2(SO_4)_3$	Langbeinite
ATAF2	0.55	Sealed curing at 60 °C	Surface	$Na_3Al(SO_4)_3$	Sodium aluminium sulfate
				$K_2Mg_2(SO_4)_3$	Langbeinite
ATAF2	0.55	Sealed curing at 60 °C	Middle	$Na_3Al(SO_4)_3$	Sodium aluminium sulfate
				$K_2Mg_2(SO_4)_3$	Langbeinite
ACSH	0.42	Sealed curing at 20 °C	Surface	$Na_3Al(SO_4)_3$	Sodium aluminium sulfate
				$K_2Mg_2(SO_4)_3$	Langbeinite
ACSH	0.42	Sealed curing at 20 °C	Middle	$Na_3Al(SO_4)_3$	Sodium aluminium sulfate
ARSH	0.42	Sealed curing at 60 °C	Surface	$Na_3Al(SO_4)_3$	Sodium aluminium sulfate
				$K_2Mg_2(SO_4)_3$	Langbeinite
ARSH	0.42	Sealed curing at 60 °C	Middle	$Na_3Al(SO_4)_3$	Sodium aluminium sulfate

4. Conclusions

The main results from this investigation on the sulfate resistance of alkali activated, natural pozzolan concrete are summarised as follows:

(1) The absorption percent of AANP concrete after exposure in sulfate solution is greater than 5.1 % but less than 7 % of the weight.
(2) Samples that were fog cured show a higher percentage of absorption. This phenomenon may be related to the retention of water by the geopolymer matrix giving rise to a more open microstructure in this type of concrete.
(3) The maximum expansion was recorded for AANP concrete in this investigation at 0.074 % after 6 months immersion in sulfate solution.
(4) The maximum loss of compressive strength for sulfate cured AANP concrete was 19.5 % following 2 years immersion in sulfate solution.

Acknowledgments

Open Access

References

ASTM C 1012-95a. (1995). standard test method for length change of hydraulic-cement mortars exposed to a sulfate solution, American Society for Testing and Materials, PA.

Bakharev, T. (2005). Durability of geopolymer materials in sodium and magnesium sulfate solutions. *Cement and Concrete Research, 35*, 1233–1246.

Bakhareva, T., Sanjayana, J. G., & Cheng, Y. B. (2002). Sulfate attack on alkali-activated slag concrete. *Cement and Concrete Research, 32*, 211–216.

Bondar, D. (2009). Alkali activation of Iranian natural pozzolans for producing geopolymer cement and concrete. A dissertation submitted to University of Sheffield in fulfilment of the requirements for the degree of Doctor of Philosophy, UK.

Bondar, D., Lynsdale, C. J., Milestone, N. B., & Hassani, N. (2012). Oxygen and chloride permeability of alkali activated natural pozzolan concrete. *ACI Materials, 109*(1), 53–62.

Bondar, D., Lynsdale, C. J., Milestone, N. B., Hassani, N., & Ramezanianpour, A. A. (2011a). Effect of type, form and dosage of activators on strength of alkali-activated natural pozzolans. *Cement and Concrete Composites, 33*(2), 251–260.

Bondar, D., Lynsdale, C. J., Milestone, N. B., Hassani, N., & Ramezanianpour, A. A. (2011b). Engineering properties of alkali-activated natural pozzolan concrete. *ACI Materials, 108*(1), 64–72.

Chotetanorm, C., Chindaprasirt, P., Sata, V., Rukzon, S., & Sathonsaowaphak, A. (2013). High-calcium bottom ash geopolymer: Sorptivity, pore size, and resistance to sodium sulfate attack. *Journal of Materials in Civil Engineering, 25*(1), 105–111.

Ezatian, F. (2002). Atlas of igneous rocks: Classification and nomenclatures. Ministry of Industries and Mines, Geological Survey of Iran (GSI) (in Farsi).

Ganjian, E., & Pouya, H. S. (2005). Effect of magnesium and sulfate ions on durability of silica fume blended mixes exposed to the seawater tidal zone. *Cement and Concrete Research, 35*, 1332–1343.

Hakkinen, T. (1986) Properties of alkali activated slag concrete. VTT Research Notes, Technical Research Centre of Finland (VTT), Finland, No. 540.

Hakkinen, T. (1987). Durability of alkali activated slag concrete. *Nordic Concrete Research, 6*, 81–94.

Neville, A. M. (1995). *Properties of concrete*. Essex, UK: Pearson Educational Limited.

Rangan, B. V. (2008). Fly ash-based geopolymer concrete, available at: http://www.yourbuilding.org/display/yb/Fly+Ash-Based+Geopolymer+Concrete. Accessed 2011.

RILEM CPC-11.2. (1994) Absorption of water by concrete by capillarity QTC14-CPC, 1982, RILEM technical recommendations for the testing and use of construction materials, International Union of Testing and Research Laboratories for Materials and Structures, E and FN Spon, UK.

Shi, C., Krivenko, P. V., & Roy, D. (2006). *Alkali-activated cement and concretes*. London, UK: Taylor & Francis.

Swamy, R. N. (1998). *Blended cement in construction*. London, UK: Taylor and Francis.

Turker, F., Akoz, F., Koral, S., & Yuzer, N. (1997). Effect of magnesium sulfate concentration on the sulfate resistance on mortars with and without silica fume. *Cement and Concrete Research, 27*, 205–214.

Zuhua, Z., Xiao, Y., Huajun, Z., & Yue, C. (2009). Role of water in the synthesis of calcined kaolin-based geopolymer. *Applied Clay Science, 43*, 218–223.